Hindawi
Advances in Materials Science and Engineering
Volume 2022, Article ID 3072663, 14 pages
https://doi.org/10.1155/2022/3072663

Research Article

Gorilla Troops Optimizer Combined with ANFIS for Wire Cut EDM of Aluminum Alloy

Elango Natarajan,[1] **V. Kaviarasan**,[2] **Wei Hong Lim**,[1] **S. Ramesh**,[3] **K. Palanikumar**,[4] **T. Sekar**,[5] **and V. H. Mok**[1]

[1]*Faculty of Engineering, Technology and Built Environment, UCSI University, Kuala Lumpur, Malaysia*
[2]*Department of Mechanical Engineering, Sona College of Technology, Salem, India*
[3]*Department of Mechanical Engineering, Jerusalem College of Engineering, Chennai, India*
[4]*Department of Mechanical Engineering, Sri Sairam Institute of Technology, Chennai, India*
[5]*Department of Mechanical Engineering, Government College of Technology, Coimbatore, India*

Correspondence should be addressed to S. Ramesh; ramesh1968in@gmail.com

Received 6 April 2022; Revised 19 May 2022; Accepted 10 June 2022; Published 29 June 2022

Academic Editor: Tadeusz Mikolajczyk

Wire cut EDM is a quite regularly used machining process in mechanical and electronic industries. This research has attempted to machine aluminum alloy for which experimental design was prepared using Box-Behnken design. Different combinational options of pulse-on time (P_1), pulse-off time (P_2), servo wire feed (WF), and current (I) were investigated and surface roughness after machining was observed. Collected 27 datasets were further used in Adaptive Neuro Fuzzy Inference System (ANFIS) to produce about 500 datasets. These 500 datasets are approximated data derived from experimental datasets, known as synthetic data. Data model was further developed and used in Gorilla Troops Optimizer (GTO) to locate the optimum machining parameters. With the excellent three search operators: move towards other gorillas, migrate towards unknown places, and migrate towards known places, GTO has produced the lowest surface roughness value of 0.500953 μm when the machining parameters of pulse-on time, pulse-off time, wire feed, and current values were set as 121 μs, 52 μs, 3 m/min, and 166A, respectively. To ensure the accuracy of the synthetic data-based model and optimality, verification and validation were conducted. Wilcoxon signed rank test was conducted for the pairwise comparison of GTO with each of its competing algorithms at the significance level of $\sigma = 0.05$. Friedman test was conducted to calculate the average ranking of each algorithm and to detect the global differences between all compared algorithms. Outperforming performance by GTO algorithm in machining of the selected material is found.

1. Introduction

Among unconventional machining processes available, wire cut electric discharge machining (WEDM) is much effective process to prepare intricate shapes and delicate objects. This thermal erosion method uses the localized thermal energy to remove the material from the substrate metal. The supply of current and voltage to electrode produces plasma between the substrate metal and tool. A small amount of heat is transferred to the substrate metal to melt and evaporate. Besides, the electrolyte used in the process removes the machined metals away from the machine. Swift toggling of pulse-on time (P_1) and pulse-off time (P_2) causes fast heating and cooling effects over the surface. This advantage of WEDM has attracted this process to use for supper alloys, hard-cutting metals, and conductive materials. Khan et al. [1] investigated machining of ASTM A572-grade 50 steel, where grey rational analysis (GRA) was used to locate the optimal machining condition. Abbasi et al. [2] also attempted the same material and analyzed it to report that pulse-on time is the predominant parameter for surface finish. Takayama et al. [3] developed a high precision rotary table with many sensors to detect wire breakage, water leakage, and machining quality. The erosion of metal

destabilizes at some depth of cutting due to accumulation of debris and it affects the process time. Ayesta et al. [4] used camera vision system to monitor the debris removal. They reported that debris removal is affected by the process parameters and hence optimal process parameters must be used not only to have high surface finish, but also to have high debris removal rate. Since electrolyte is important in this process, kerosene oil, EDM oil, and distilled water were also evaluated by hazard and operability analysis [5]. They revealed that aerosol concentration and dielectric consumption affect the environment and hence new dielectric fluid must be invented. Liu et al. [6] developed a pulse power source to avoid back-off error, which occurs in WEDM of semiconductors as discharge of silicon affects the servo controller. Newly developed power source has stabilized the discharge probability. Significant research contributions [7–25] in the recent years are reviewed and listed in Table 1.

Alam et al. [26] recently reviewed optimization of WEDM parameters, in which they detailed the past published research using GRA and RSM methods. Abidi et al. [27] used MOGA-II algorithm to optimize the parameters to machine nickel-titanium-based shape memory alloy. At this end, it is acknowledged that only minimal research has been conducted in finding the best machining condition using optimization algorithm.

Metaheuristic algorithms are more efficient in locating the optimal solutions for single or multiobjective problems [28, 29] and hence Gorilla Troops Optimizer (GTO) is attempted in this research to search for optimal solution in machining of Al alloy. In a brief of method of research, experiments were conducted using L_{27} orthogonal array. Surface roughness of machined samples and their respective cutting parameters were used to develop an Adaptive Neuro Fuzzy Inference System (ANFIS) from which about 500 synthetic data were further generated. Response surface model (RSM) was developed with these data and applied to GTO algorithm to locate the optimal process parameters. At this end, the paper is organized as below; Section 2 presents the material, experimentation, ANFIS model, and GTO algorithm, while Section 3 presents and discusses the results, while conclusion of current research is presented in Section 4.

2. Materials and Methods

2.1. Materials. Aluminum 7075 alloy was the material investigated in this research, as this material is the most suitable material for structural application including transport, aerospace, marine, and defence. Aluminum alloys are famous for their mechanical properties and weight-strength ratio. Machining this alloy using a conventional machining process does not result in the dimensional accuracy every time. Besides, rejection of parts is also there due to no align with near net shape. WEDM is one of the unconventional machining processes that perfectly suits this scenario and gives better surface finish. Mechanical properties and chemical properties of Al7075 alloy are listed in Tables 2 and 3, respectively.

2.2. Experimentation. Al7075 alloy plate in 200 mm × 150 mm × 10 mm and WEDM SPRINTCUT model with CNC control was used for experimentation. Brass wire electrode of 0.25 mm diameter was used as cathode and deionised water was used as the dielectric fluid. Initially, the plate was machined using arbitrary chosen parameter setting to identify the sparking condition and wire breakage. After conducting a few preliminary experiments, the parameter setting range was fixed for pulse-on time (P_1), pulse-off time (P_2), servo wire feed (WF), and current (I) as shown in Table 4. Box-Behnken design (BBD) is the best method for threelevel design [25] and hence design of experiments (L_{27} DoE) was prepared using BBD. The machining was carried out as per DoE and surface roughness was measured in three different locations using surface roughness tester (Mitutoyo make Surftest 211). Figure 1 shows the machining and machined samples, while Table 5 reports the experimental results.

ANOVA, a statistical tool, was used to find the goodness of fit of the experimental data. The two-way ANOVA with 95% confidence level was carried out as the value of probability <5% is considered significant. Table 6 shows the results from ANOVA. Each parameter and cross product of parameters are found significant. The model is significant with $R^2 = 99.41\%$ and standard deviation = 0.0201349.

2.3. Adaptive Neurofuzzy Inference System (ANFIS). ANFIS is a soft computing technique that utilizes artificial neural network (ANN) and fuzzy logic theory to predict the data samples. It is a simple and accurate adaptive technique to build a prediction model. The reason for using ANFIS in this research is that we wanted to generate as many datasets as possible from a small size of experimental data (27 datasets). Two-tier approach of using ANFIS and RSM was tested and reported as a better method [30]. Optimal searching was more accurate when data population was large. Hence, the above tabulated twenty-seven datasets were used in ANFIS for training the Neurofuzzy Interference System, which could result in plentiful datasets.

ANFIS has different types of membership function (MF) such as triangular shaped membership function (trimf), trapezoidal-shaped membership function (trapmf), generalized bell-shaped membership function (gbellmf), Gaussian curve membership function (gaussmf), Gaussian combination membership function (gauss2mf), P-shaped membership function (pimf), difference between two sigmoidal membership functions (dsigmf), and product of two sigmoid membership functions (psigmf). We attempted all these MFs to build predictive models and finally selected generalized bell-shaped membership function (gbellmf) based on minimum root mean square error (RMSE). This MF is Sugeno type IF-THEN rules to predict the outcomes. RMSE value observed in each model is listed as Trimf model = 1.1394, Trapmf model = 1.1696, Gbelmf model = 0.9605, Gausmf model = 0.9701, Gaus2mf model = 1.1677, Sigmf model = 0.832, Dsigmf model = 1.1672, Psigmf model = 1.1666, Pimf model = 1.7280, Smf model = 1.1728, and Zmf model = 1.1728.

Training of model was done with 27 experimental data. Six additional experiments were conducted with arbitrarily

Table 1: Significant published articles on WEDM in recent years.

Reference	Material used	Contribution
[7]	Al6061/SiC/graphite	Brass wire, zinc coated wire, and diffused coated wires were investigated based on the speed. They reported that diffused coated wire is the best of these wire materials.
[8]	Carbon steel 1017 and aluminum alloy 6060	Wire feed rate (3, 5 and 7 mm/minute) was investigated and it was reported that low feed rate is the best to improve the surface finish.
[9]	High speed steel (HSS) M2 grade	Material removal rate, surface roughness, and width of kerf were analyzed using GRA. They used tool makers' microscope to measure the amount of material wasted during machining, known as kerf width.
[10]	Titanium alloy	Cause of wire rupture which subsequently affects the production and productivity was investigated. They reported that stay of debris caused by low flushing pressure and high wire tension caused by instantaneous high temperature during the machining are two major reasons for wire rupture.
[11]	Friction stir welded 5754 aluminum alloy	RSM was used to optimize the process variables in machining friction stir welded 5754 aluminum alloy.
[12]		Dry cutting, cryogenic cutting, minimum quantity lubrication (MQL), nanocutting fluids, and MQL nanofluids were investigated and it was reported that MQL nanofluid and cryogenic machining showed the best sustainable strategies.
[13]	LM13 aluminum alloy	Slotted copper tool was used to drill aluminum alloy and it was reported that modified tool design has given higher surface finish and material removal rate.
[14]	AISI 304 stainless steel	The influence of various parameters was investigated and it was reported than wire tension influences greatly the surface finish, removal rate, and microhardness of the material. It does not influence the kerf width.
[15]	High carbon high chromium steel	Zirconium powder mixed dielectric fluid was used and it was reported that it has improved the performance of the machining.
[16]	Pure titanium	Multiresponse optimization was conducted using integrated approach of RSM and GRA. They reported the optimal parameters are $T_{on} = 6\mu s$, $T_{off} = 4\mu s$, and discharge current = 6A.
[17]	LM13 Al alloy/10ZrB2/5TiC hybrid composite	Multiresponse optimization was conducted using RSM and GRA. Their aim was to investigate the effect of process parameters on material removal rate (MRR), electrode wear rate (EWR), and overcut (OC). They finally reported that current is the highly influencing parameter on these responses.
[18]	AZ61 magnesium alloy /B_4C/SiC hybrid composite	The influencing parameter among percentage of filler reinforcement, stirring speed, time of stirring, and process temperature.
[19]	Al-Si12/B4C/Fly ash hybrid composite	Material removal rate was investigated and it was reported that it highly depends on pulse-on time and fly ash reinforcement.
[20]	AA1050/5 wt.% SiC composite	Zinc coated copper wire was used to machine SiC reinforced aluminum composite and it was reported that open voltage is the significant parameter.
[21]	Monel K-500, a nickel–copper based alloy	WEDM was applied to super alloy machining. Pulse-on time and pulse-off time affect cutting rate proportionally and inverse proportionally, respectively. Spark gap decreases the cutting rate and surface roughness.
[22]	Inconel-800 superalloy	Trapezoidal interval type-2 fuzzy numbers were applied for handling the uncertainties associated with the subjective assessment of the criteria. The integration of T2FS with additive ratio assessment (ARAS) method resulted in the best WEDM process parameters.
[23]	Cemented carbide	This research attempted to compare edges made using WEDM techniques and conventional edges made in the grinding process.
[24]	Ti6Al4V alloy	This work combines integrated fuzzy analytic hierarchy process (AHP) and fuzzy technique for order preference by similarity to ideal situation (TOPSIS) to optimize the WEDM process.
[25]	AZ31 alloy	They used Box-Behnken design (BBD) to conduct experiments and multiobjective particle swarm optimization (MOPSO) to optimize cutting rate and recast layer.

selected input parameters and these data as shown in Table 7 were used for testing the ANFIS model. Once training and testing of ANFIS model were completed, about 500 datasets were generated from the ANFIS model. These 500 datasets were used to build a response surface methodology (RSM) model shown below.

$$\begin{aligned} R_a = {} & -190.05 + 2.037P_1 + 2.595P_2 - 3.699WF - 0.0353I \\ & - 0.006571P_1^2 - 0.06374P_2^2 + 0.22117WF^2 - 0.005201I^2 \\ & - 0.006053P_1 \times P_2 + 0.02109P_1 \times WF - 0.000594P_1 \\ & \times I - 0.00083\,P_2 \times WF + 0.03226P_2 \times I. \end{aligned} \quad (1)$$

Table 2: Mechanical properties of aluminum 7075 alloy.

Property	Value
Density	2.81 g/cc
Ultimate tensile strength	572 MPa
Modulus of elasticity	71.7 GPa
Brinell hardness	150
Fatigue strength	159 MPa
Machinability	70%
Thermal conductivity	130 W/m-k
Melting point	477–635°C
Electrical resistivity	5.15×10^{-006} ohm-cm

Table 3: Chemical composition of aluminum 7075 alloy (as received from the supplier).

Al	Si	Fe	Cu	Mn	Mg	Cr	Zn	Ti	Others
86.77	0.4	0.5	2.0	0.3	2.9	0.28	6.1	0.2	0.15

All values mentioned in wt%.

Table 4: Machining parameters and fixed levels.

Machining parameter	Levels		
	I	II	III
Pulse-on time (P_1 in μs)	120	125	130
Pulse-off time (P_2 in μs)	50	55	60
Servo wire feed (WF in m/min)	1	2	3
Current (I in ampere)	150	160	170

2.4. Gorilla Troops Optimizer (GTO). Gorilla Troops Optimizer (GTO) is one of the emerging metaheuristic search algorithms proposed by Abdollahzadeh et al. [31] in 2021 to solve global optimization problems, where its search mechanisms are essentially inspired by the collective behavior and social intelligence of gorilla life in nature. Similar to other species of apes, gorillas live in the troops consisting of an adult male gorilla known as silverback, multiple female and male gorillas, and offspring. Silverback refers to the strongest gorilla with unique silver-colored hair on its back and it is considered as troop leader that is responsible for decision making and conflict resolution, as well as spearheading other troop activities such as food searching and strategic retreat for troop safety. On the contrary, other male gorillas that do not have silver-colored hair on their back are relatively weaker and hence affiliated to silverback as the backup defenders of troops. Five typical behaviors are generally observed from gorilla troops to enable the formulation of search operators with different exploration and exploitation strengths. These behaviors include the moving to other gorillas, migration to unknown areas, migration to the surrounding of known areas, staying in original troop to follow silverback, and competition to mate with female gorillas upon the decease of silverback. Similar to other metaheuristic search algorithms, the optimization process using GTO can be expressed in three main stages, i.e., population initialization, exploration phase, and exploitation phase as explained in next subsections.

2.4.1. Population Initialization. Suppose that a group of gorillas with population size of N is used to solve a given optimization problem with dimensional size of D. The position of each i-th gorilla in solution space at any t-th iteration is considered as a potential solution and expressed as $X_i(t) = [x_{i,1}(t), \ldots, x_{i,d}(t), \ldots, x_{i,D}(t)]$, where $i = 1, \ldots, N$ and $d = 1, \ldots, D$ represent the population index of gorilla and dimensional index of problem, respectively. Let LB and UB be the lower and upper boundary limits of solution, respectively. At $t = 0$, the position value of every i-th gorilla, i.e., $X_i(0)$, can be initialized as

$$X_i(0) = LB + r_1 \times (UB - LB), \tag{2}$$

where $r_1 \in [0, 1]$ is a real-valued number randomly generated from uniform distribution.

2.4.2. Exploration Phase. From the perspective of metaheuristic search algorithms, an exploration process is essential in early stage of optimization to enable the population for discovering the unvisited regions in solution space. For the exploration phase of GTO, three search operators are incorporated by emulating different behaviors of gorilla troops, i.e., move towards other gorillas, migrate towards unknown places, and migrate towards known places.

Define $p \in [0, 1]$ as a constant parameter used to indicate the likelihood of i-th gorilla to migrate towards unknown places and $rand \in [0, 1]$ as a real-valued number randomly generated from uniform distribution. If $rand < p$, the i-th gorilla chooses migration towards an unknown region to further enhance the exploration strength of GTO. For the scenario of $rand \geq 0.5$, the i-th gorilla tends to move towards a randomly selected gorilla denoted as $X_r(t)$ to attain good balancing of exploration and exploitation searches. Finally, the i-th gorilla chooses migration towards a known region to maintain good population diversity when $rand < 0.5$. Let $GX_r(t)$ be candidate position of a randomly selected gorilla created in the t-th iteration, whereas $GX_i(t+1)$ refers to the candidate position of each i-th gorilla created in the next $(t+1)$-th iteration. Define $r_2, r_3 \in [0, 1]$ as two real-valued numbers randomly generated from uniform distribution; then

$$GX_i(t+1) = \begin{cases} r_1 \times (UB - LB) + LB, rand < p, \\ (r_2 - C) \times X_r(t) + L \times Z \times X_i(t), rand \geq 0.5, \\ X_i(t) - L \times \{L \times [X_i(t) - GX_r(t)] + r_3 \times [X_i(t) - GX_r(t)]\}, rand < 0.5. \end{cases} \tag{3}$$

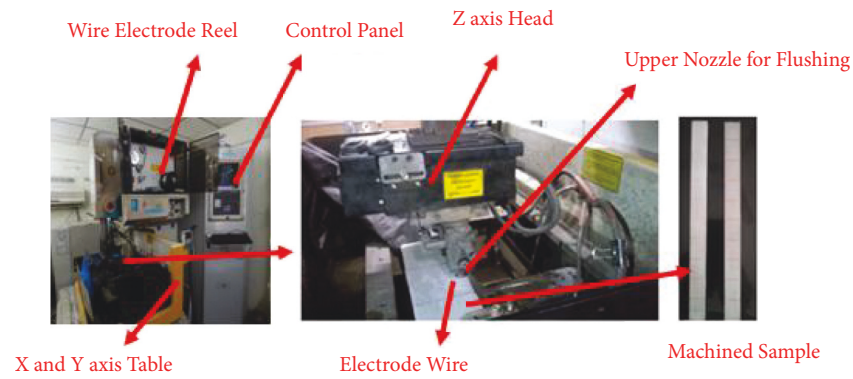

Figure 1: WEDM machining and machined sample.

Table 5: Experimental results.

Expt. No	Pulse-on time, P_1 (μs)	Pulse-off time, P_2 (μs)	Servo wire feed, WF (m/min)	Current, I (A)	Surface roughness, R_a (μm)
1	120	50	1	150	1.92
2	120	50	2	160	1.77
3	120	50	3	170	1.56
4	120	55	1	160	1.85
5	120	55	2	170	1.77
6	120	55	3	150	1.47
7	120	60	1	170	2.06
8	120	60	2	150	1.99
9	120	60	3	160	1.76
10	125	50	1	150	2.22
11	125	50	2	160	2.09
12	125	50	3	170	1.82
13	125	55	1	160	1.97
14	125	55	2	170	1.90
15	125	55	3	150	1.78
16	125	60	1	170	1.98
17	125	60	2	150	2.13
18	125	60	3	160	1.92
19	130	50	1	150	2.21
20	130	50	2	160	2.10
21	130	50	3	170	1.78
22	130	55	1	160	1.77
23	130	55	2	170	1.73
24	130	55	3	150	1.85
25	130	60	1	170	1.64
26	130	60	2	150	1.96
27	130	60	3	160	1.77

The parameters of C, L, and Z presented in equation (3) can be calculated as follows:

$$C = \left[\cos\left(2 \times r_4\right) + 1\right] \times \left(1 - \frac{t}{T_{\max}}\right), \tag{4}$$

$$L = C \times l, \tag{5}$$

$$Z \in [-C, C], \tag{6}$$

where $\cos(.)$ is a cosine operator; $T_{\max}$ is the maximum iteration numbers set for GTO; $r_4 \in [0, 1]$ and $l \in [-1, 1]$ are the real-valued numbers randomly generated from uniform distribution. Equation (4) is used to simulate the tendency of GTO to perform searching with larger interval of changes in the earlier stage of optimization process and these search ranges are gradually reduced in later stage. Meanwhile, equation (5) is designed to emulate the variation of silverback's leadership throughout the optimization process.

Upon the completion of exploration phase, the candidate position of each i-th gorilla is obtained as $GX_i(t+1)$ and its fitness value is evaluated as $F[GX_i(t+1)]$. The current fitness value of each i-th gorilla, i.e.,$F[X_i(t)]$, is then compared with $F[GX_i(t+1)]$. The new candidate position $GX_i(t+1)$ is used to update the current position $X_i(t)$ if the former solution has more superior fitness. Otherwise, the

Table 6: Results from ANOVA.

Source	Degrees of freedom (DF)	Adj SS	Adj MS	F-value	P-value	Remarks
Model	13	0.885626	0.068125	168.04	0.000	Significant
Linear	4	0.191479	0.047870	118.08	0.000	
P_1	1	0.024200	0.024200	59.69	0.000	
P_2	1	0.003756	0.003756	9.26	0.009	
WF	1	0.111111	0.111111	274.07	0.000	
I	1	0.019136	0.019136	47.20	0.000	
Square	4	0.278777	0.069694	171.91	0.000	
$P_1 \times P_1$	1	0.131030	0.131030	323.20	0.000	
$P_2 \times P_2$	1	0.115741	0.115741	285.49	0.000	
WF × WF	1	0.029606	0.029606	73.03	0.000	
I × I	1	0.000735	0.000735	1.81	0.201	
2-Way	5	0.270307	0.054061	133.35	0.000	
$P_1 \times P_2$	1	0.136533	0.136533	336.78	0.000	
$P_1 \times$ WF	1	0.056033	0.056033	138.21	0.000	
$P_1 \times$ I	1	0.064533	0.064533	159.18	0.000	
$P_2 \times$ WF	1	0.011756	0.011756	29.00	0.000	
$P_2 \times$ I	1	0.000450	0.000450	1.11	0.311	
Error	13	0.005270	0.000405			
Total	26	0.890896				

Standard deviation = 0.0201349 $R^2 = 99.41\%$, R^2(adj) = 98.82%, R^2(pred) = 96.67%.

Table 7: Test datasets used in ANFIS model.

Expt. No Units	Puls-on P_1 (μs)	Pulse-off P_2 (μs)	Wire feed rate WF (m/min)	Current I (A)	Surface roughness R_a (μm)
1.	122	52	1	155	2.06
2.	122	52	2	165	1.66
3.	124	54	3	165	1.98
4.	124	54	1	155	2.01
5.	126	56	2	165	1.69
6.	126	56	3	155	1.88

solution $GX_i(t+1)$ is discarded if it has more inferior fitness. Similar mechanism is used to update the position of silverback $X_{\text{silverback}}(t)$ by comparing its fitness value of $F[X_{\text{silverback}}(t)]$ with that of $F[GX_i(t+1)]$.

2.4.3. Exploitation Phase. On the contrary to exploration, exploitation has crucial role in the later stage of optimization process because it can further refine the solutions found in promising regions of search space. For the exploitation phase of GTO, two search operators are designed by simulating the behaviors of gorilla troops to follow the silverback for food searching and to compete for mating with the adult female gorillas.

Suppose that W is a parameter used to determine the behavior of each i-th gorilla in exploitation phase and C is a parameter obtained from equation (4). When $C \geq W$, the i-th gorilla chooses to obey the instructions of silverback in exploitation phase and its candidate position at the next $(t+1)$-th iteration; i.e., $GX_i(t+1)$, is updated as follows:

$$GX_i(t+1) = L \times M \times [X_i(t) - X_{\text{silverback}}(t)] + X_i(t), \quad (7)$$

where L is a parameter obtained from equation (5); $X_{\text{silverback}}(t)$ refers to the position of silverback at the t-th iteration. Meanwhile, the parameter M in equation (7) is calculated as

$$M = \left(\left| \frac{1}{N} \sum_{i=1}^{N} GX_i(t) \right|^{2^L} \right)^{1/2^L}, \quad (8)$$

where N refers to population size of GTO; $GX_i(t)$ represents the candidate position of each i-th gorilla at the current t-th iteration.

On the contrary, the i-th gorilla tends to compete with other male gorillas for mating with the adult female gorillas during exploitation phase if $C < W$. The mathematical models used to simulate this behavior are formulated as

$$GX_i(t+1) = X_{silverback}(t) - [X_{silverback}(t) \times Q - X_i(t) \times Q] + A, \quad (9)$$

where Q represents the impact force; A is a vector used to indicate the degree of violence encountered in competition. Both of Q and A can be computed as

$$Q = 2 \times r_5 - 1, \quad (10)$$

$$A = \beta \times E, \quad (11)$$

$$E = \begin{cases} N_1, r_6 \geq 0.5 \\ N_2, r_6 < 0.5 \end{cases}, \quad (12)$$

where $r_5, r_6 \in [0, 1]$ are two real-valued numbers randomly generated from uniform distribution; β is a constant; E is used to simulate the violence effect on each dimension of solution based on two normal distributions of N_1 and N_2. If$r_6 \geq 0.5$, E is assigned as an array with size of$1 \times D$, where N_1 is used to randomly generate different values for each dimension. On the other hand, only a single random number is generated by N_2 and assigned to E when $r_6 < 0.5$.

Similar with exploration phase, the fitness value of each i-th gorilla's candidate position $GX_i(t+1)$ is evaluated as $F[GX_i(t+1)]$ and then compared with the current fitness $F[X_i(t)]$. If $GX_i(t+1)$ has more superior fitness than $X_i(t)$, the latter solution will be replaced by the former one. Otherwise, $GX_i(t+1)$ will be discarded due to its inferior fitness. Similar mechanism is also used to update the position of silverback $X_{\text{silverback}}(t)$ by comparing its fitness value of $F[X_{\text{silverback}}(t)]$ with that of $F[GX_i(t+1)]$.

2.4.4. Overall Search Mechanisms of GTO. The overall search mechanisms of GTO are presented in Figure 2. Initially, the population of GTO is randomly generated by using uniform distribution. Both of the exploration and exploitation phases are switched alternately during the optimization process of GTO. For exploration phase, three different search operators can be used to determine the candidate position of every i-th gorilla. Meanwhile, two different search operators are devised in exploitation phase to update the candidate position of every i-th gorilla. It is notable that greedy selection is used to update the current position of each i-th gorilla and position of silverback for both exploration and exploitation phases. The iterative search processes of GTO in exploration and exploitation phases are repeated until the predefined termination condition, i.e., current iteration exceeding maximum iteration ($t > T_{\max}$), is satisfied. At the end of optimization process, the silverback's position, i.e., $X_{\text{silverback}}(T_{\max})$, is returned as the best solution to solve given problem. Due to the promising optimization performance of GTO, it has been applied to solve some real-world optimization problems such as feature selection [32], image segmentation [33], and parameter estimation of fuel cell [34] and solar panel [35]. To the best of authors' knowledge, the feasibility of GTO to solve machining optimization problem is one of the areas that remains unexplored.

3. Performance Evaluation of Proposed WEDM Machining Optimization Problem

3.1. Simulation Settings of All Compared Algorithms. Extensive simulation studies are conducted to evaluate the performance of GTO in solving the proposed WEDM machining optimization problem. The simulation results produced by GTO are then compared with another six metaheuristic search algorithms known as particle swarm optimization (PSO) [36], differential evolution (DE) [37], teaching learning-based optimization (TLBO) [28], grey wolf optimizer (GWO) [38], sine cosine algorithm (SCA) [39], and arithmetic optimization algorithm (AOA) [40]. The optimal parameter settings of all compared algorithms are determined based on the recommendations in their respective literature as shown in Table 8 and original source codes are obtained from their authors to ensure fair comparison. The same population size of $N = 10$ and maximum iteration numbers of $T_{\max} = 100$ are also set to ensure all seven metaheuristic algorithms are compared in fair manner. When solving real-world optimization problem such as WEDM machining considered in current study, it is essential to achieve proper tradeoff between the solution accuracy and computational overhead of algorithm. Although it is more likely for metaheuristic search algorithm such as GTO to obtain the solutions with better accuracy when larger population size is set, the computational complexity of algorithm is estimated as $O(N \times (1 + T_{\max} + T_{\max} D) \times 2)$ [31] using Big-O notation that tends to increase with population size, where N, $T_{\max}$, and D refer to the population size, maximum iteration numbers, and total dimensional size of problems, respectively. The increasing computational complexity of GTO is undesirable and not computationally feasible for real-world optimization problems. Furthermore, our simulation studies indicate that GTO can solve the WEDM machining optimization problems with better accuracy than other competing algorithms when the population size of $N = 10$ is set. This is a crucial finding to reveal the competitive optimization performances of GTO when solving real-world optimization problems. In order to alleviate the random discrepancy issue, all compared algorithms are simulated independently for 20 runs under the same simulation environment of Matlab (R2021a) installed in a personal computer with Intel® Core™ i5-7400 CPU processor with 24.0 GB RAM when solving the proposed WEDM machining optimization problems.

3.2. Simulation Results and Discussion. The optimal machining parameters (i.e., pulse-on time, pulse-off time, wire feed, and current values) obtained by GTO and their corresponding response variable of surface roughness (R_a) when solving the proposed WEDM machining optimization problems for 20 consecutive times are presented in Table 9. The number of iteration numbers T_{best} consumed by GTO to achieve the best machining result in every simulation run is also recorded in Table 9. Accordingly, GTO is able to consistently search for the optimal values of pulse-on time, pulse-off time, wire feed, and current that lead to the low values of surface roughness. It is also noteworthy that GTO has consumed an average iteration number of 24 to find the optimal machining parameters in these 20 simulations runs, implying the promising search efficiency of this algorithm. From Table 9, it is observed that GTO has produced the lowest surface roughness value of 0.500953 μm when the machining parameters of pulse-on time, pulse-off time, wire feed, and current values are set as 121 μs, 52μs, 3 m/min, and 166 A, respectively, at the 18th simulation run with 8 iterations and 19th simulation run with 15 iterations. These optimal machining parameters are further validated by measuring the experimental value of surface roughness as 0.500μm, i.e., only 0.2% of deviation from the predicted

Algorithm 1: GTO

Inputs: N, D, T_{max}, LB, UB, p, W, β

Initialize $t = 0$, $X_{silverback}(0) \leftarrow \emptyset$, $F[X_{silverback}(t)\,] \leftarrow \infty$;
for each i-th gorilla **do** /*Population Initialization*/
  Randomly generate $X_i(0)$ using Eq. (2);
  Evaluate the fitness of $X_i(0)$ as $F[X_i(0)]$;
  $GX_i(0) \leftarrow X_i(0)$, $F[GX_i(0)] \leftarrow F[X_i(0)]$
  if $F[GX_i(0)]$ *is superior to* $F[X_{silverback}(0)]$ **then**
    $X_{silverback}(0) \leftarrow GX_i(0)$, $F[X_{silverback}(t)\,] \leftarrow F[GX_i(0)]$;
  end if
end for
while $t \le T_{max}$ **do** /*Main Loop*/
  Update C, L and Z using Eqs. (4), (5) and (6), respectively;
  for each i-th gorilla **do** /*Exploration*/
    Update $GX_i(t+1)$ using Eq. (3);
    Evaluate the fitness of $GX_i(t+1)$ as $F[GX_i(t+1)]$;
    if $F[GX_i(t+1)]$ *is superior to* $F[X_i(t)]$ **then**
      $X_i(t+1) \leftarrow GX_i(t+1)$, $F[X_i(t+1)] \leftarrow F[GX_i(t+1)]$
      if $F[GX_i(t+1)]$ *is superior to* $F[X_{silverback}(t)]$ **then**
        $X_{silverback}(t+1) \leftarrow GX_i(t+1)$, $F[X_{silverback}(t+1)\,] \leftarrow F[GX_i(t+1)]$;
      end if
    end if
  end for
  for each i-th gorilla **do** /*Exploitation*/
    if $C \ge W$ **then**
      Update $GX_i(t+1)$ using Eqs. (7) and (8);
    else
      Update $GX_i(t+1)$ using Eqs. (9) to (12);
    end if
    Evaluate the fitness of $GX_i(t+1)$ as $F[GX_i(t+1)]$;
    if $F[GX_i(t+1)]$ *is superior to* $F[X_i(t)]$ **then**
      $X_i(t+1) \leftarrow GX_i(t+1)$, $F[X_i(t+1)] \leftarrow F[GX_i(t+1)]$
      if $F[GX_i(t+1)]$ *is superior to* $F[X_{silverback}(t)]$ **then**
        $X_{silverback}(t+1) \leftarrow GX_i(t+1)$, $F[X_{silverback}(t+1)\,] \leftarrow F[GX_i(t+1)]$;
      end if
    end if
  end for
  $t \leftarrow t+1$;
end while

Outputs: $X_{silverback}(T_{max})$, $F[X_{silverback}(T_{max})\,]$

Figure 2: Pseudocode of GTO.

value of surface roughness. Given the small performance difference, it can be concluded that there is good consistency between the simulated and actual results.

Table 10 presents the best, worst, mean, and standard deviation (SD) values of surface roughness obtained by all compared seven metaheuristic search algorithms when solving the proposed WEDM machining optimization problems for 20 consecutive times. The best (i.e., lowest) surface roughness values produced by each algorithm are highlighted in bold. Although there are four algorithms (i.e., PSO, DE, TLBO, and GTO) that are able to produce the lowest values, GTO is the only algorithm that can solve the proposed WEDM machining optimization problems with the lowest values of worst and mean surface roughness. The promising performance of GTO to consistently solve the WEDM machining problem with low surface roughness value is also reflected from the lowest SD value. On the contrary, the optimization performances of algorithms such as PSO, DE, TLBO, and AOA are observed to be inconsistent as revealed by the inferior values of worst surface roughness and SD. These findings imply the high tendencies of PSO, DE, TLBO, and AOA to be trapped into local optima and suffer with premature convergence issues in certain trials of simulations. Although GWO and SCA can deliver more consistent performances when dealing with the proposed WEDM machining optimization problem, the overall surface roughness values obtained by these two competing algorithms are generally more inferior than those of GTO.

Figure 3 depicts the convergence curves obtained by all metaheuristic search algorithms when solving the proposed WEDM machining problem to further analyze their optimization performances in real-world application. Accordingly, each compared algorithm has exhibited different accuracy and efficiency in searching for the best combinations of machining parameters (i.e., pulse-on time, pulse-off time, wire feed, and current) that aim to minimize the surface roughness value. Among all compared metaheuristic search algorithms, AOA is identified to have worst performance because it has very slow convergence speed during the early stage of search process and its population only starts to converge towards the promising solution regions at the middle stage of optimization. The poor convergence characteristic of AOA is considered as a main contributing factor that prohibits its population to locate the global optimum in earlier stage, hence resulting in its inferior performance to solve the proposed WEDM machining problems with undesirably large surface roughness value. Although both PSO and DE have started the optimization processes with relatively lower surface roughness values, these two algorithms are observed to suffer with

Table 8: Parameter settings of all compared metaheuristic search algorithms used to solve WEDM machining optimization problems.

Algorithm	Parameter settings
PSO	Inertia weight ω: 0.9 $\longrightarrow$ 0.2, acceleration coefficients $c_1 = c_2 = 2.0$
DE	Scaling factor $F = 0.5$, crossover rate $CR = 0.9$
TLBO	Teaching factor $T_f \in \{1, 2\}$
GWO	Convergence coefficient a: 2.0 $\longrightarrow$ 0.0
SCA	Constant used to balance exploration and exploitation, $A_{SCA} = 2$
AOA	Control parameter used to adjust search process $\mu = 0.5$, control parameter used to define exploitation accuracy over iterations $\alpha = 5$
GTO	Constant parameter used to multiply with violence effect $\beta = 3$, constant parameter used to determine the behavior of gorilla in exploitation phase $W = 0.8$, constant parameter used to indicate the likelihood of gorilla to migrate towards unknown places $p = 0.03$

Table 9: Optimal machining parameters and the corresponding response variables produced by GTO in 20 consecutive simulation runs.

Run	Pulse-on time, P_1 (μs)	Pulse-off time, P_2 (μs)	Wire feed, WF (m/min)	Current, I (A)	Surface roughness, R_a (μm)	Iteration numbers to achieve best result, T_{best}
1	121	54,	3	173	0.520676	3
2	120	52	2	166	0.503164	7
3	130	50	4	164	0.501744	37
4	127	52	3	168	0.504061	35
5	121	53	1	173	0.512619	38
6	121	54	3	173	0.520676	8
7	128	53	1	173	0.500999	23
8	128	53	1	173	0.500999	45
9	120	53	3	169	0.508859	29
10	121	52	3	166	0.500953	24
11	120	53	3	169	0.508859	24
12	128	59	4	154	0.507776	12
13	120	53	3	169	0.508859	43
14	120	53	3	169	0.508859	50
15	130	50	4	164	0.501744	31
16	120	53	3	169	0.508859	12
17	120	53	3	169	0.508859	16
18	121	52	3	166	0.500953	8
19	121	52	3	166	0.500953	15
20	120	53	3	169	0.508859	19

premature convergence issues as demonstrated by the plateau regions of their convergence curves in early stage of optimization, i.e., before 20th iteration. The high tendency of PSO and DE populations to be trapped into the local optima regions can be justified by their relatively simple search mechanisms that are unable to achieve good balancing of exploration and exploitation when dealing with fitness landscapes of real-world optimization problems. The inferior performances of PSO and DE to avoid misleading information of local optima regions tend to prevent these two algorithms consistently solving the proposed WEDM machining problems with lower surface roughness values. The remaining algorithms such as TLBO, GWO, SCA, and GTO have better robustness to handle premature convergence issues as demonstrated by their convergence curves with more promising convergence characteristics and lower surface roughness values. Among these four algorithms, GTO is proven as the best performing algorithm to solve the proposed WEDM machining optimization problem because it shows fastest convergence rate and is able to locate the solution that is nearest to the global optimum. The competitive optimization performances demonstrated by GTO against TLBO, GWO, and SCA can be justified by its inherent mechanisms used to achieve proper balancing of exploration and exploitation searches of algorithm. As compared to the latter three algorithms equipped with lesser numbers of search operators, GTO is designed to have two optimization phases (i.e., exploration and exploitation) with five search operators with different exploration and exploitation strengths. Depending on the optimization stage and location of each individual solution in search space, one of the embedded search operators can be triggered and play dominant role to guide the individual solution searching towards the promising regions of search space. The excellent capability of GTO in balancing its exploration and exploitation searches enables its population to locate the global optimum of WEDM machining optimization problem rapidly without requiring large numbers of population size for effective searching.

Different nonparametric statistical procedures [41, 42] are further used for performance evaluation of all competing metaheuristic search algorithms by referring to their surface

Table 10: The best, worst, mean, and standard deviation (*SD*) values of surface roughness produced by all compared algorithms.

Algorithm	Surface roughness, R_a			
	Best	Worst	Mean	SD
PSO	**0.500953**	1.210000	0.58860	0.1672400
DE	**0.500953**	1.006769	0.53508	0.1113500
TLBO	**0.500953**	1.151530	0.53999	0.1440400
GWO	0.501744	0.570686	0.52383	0.0187180
SCA	0.501744	0.586320	0.52038	0.0195790
AOA	0.501744	0.790220	0.59673	0.0666010
GTO	**0.500953**	**0.520676**	**0.50697**	**0.0060295**

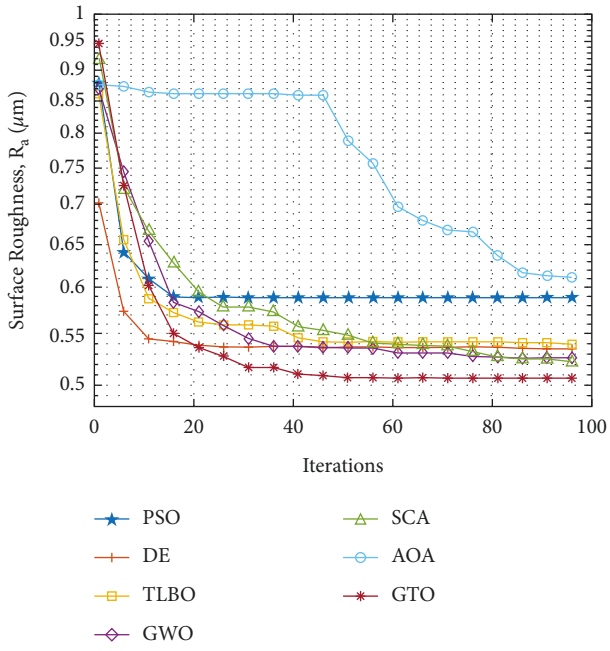

Figure 3: Convergence curves produced by all compared meta-heuristic search algorithms.

roughness values obtained. Wilcoxon signed rank test [41, 42] is employed for the pairwise comparison of GTO with each of its competing algorithms at the significance level of $\sigma = 0.05$. The results of Wilcoxon signed rank test are reported in terms of the sum of rank (i.e., R^+ anR^- d) and the associated p-values. R^+ and R^- shown in Table 11 indicate the sum of rank for GTO to perform better and perform worse than a given competing algorithm, respectively. Meanwhile, p-value is the minimum level of significance for detecting performance differences between algorithms. If $p < \sigma$, it implies the existence of strong evidence to reject null hypothesis and the best results achieved by better performing algorithms are statistically significant. The pairwise comparison results reported in Table 12 show that GTO can perform significantly better than PSO, GWO, SCA, and AOA because their corresponding p-values are all smaller than the threshold significance value of $\sigma = 0.05$. In other words, the competitive performances of GTO against PSO, GWO, SCA, and AOA are evident and not achieved by any random chances. On the other hand, there are no significance performance differences detected between GTO and

Table 11: Wilcoxon signed rank test for the pairwise comparison between GTO and its peer algorithms.

Algorithm compared with GTO	R^+	R^-	p-value
PSO	177.0	13.0	0.000900
DE	127.5	62.5	0.173118
TLBO	117.0	93.0	0.637602
GWO	185.5	24.5	0.002060
SCA	171.5	18.5	0.001844
AOA	208.0	2.0	0.000104

DE as well as GTO and TLBO as indicated by their relatively large p-values. This implies that the poor performances of DE and TLBO might only happen in certain simulation runs. GTO is still considered as a better performing algorithm due to excellent consistency to solve the proposed WEDM machining optimization problem with low surface roughness values.

Multiple comparison analyses [41, 42] are also conducted for more thorough evaluations of GTO and its competing algorithms. Friedman test was first employed to calculate the average ranking of each algorithm and detect the global differences between all compared algorithms. As reported in Table 12, GTO with lowest average rank value emerges as the best performing algorithm to solve the proposed WEDM problem with lowest surface roughness values. The remaining compared algorithms are ranked as follows: TLBO, DE, SCA, GWO, PSO, and AOA. The p-value presented in Table 12 also detects the significant global differences between all compared algorithms because $p < \sigma$, where $\sigma = 0.05$ is defined as the threshold significance level. Referring to the findings from Friedman test, another three post hoc analyses known as Bonferroni-Dunn, Holm, and Hochberg methods are employed to further compare the performance differences between GTO and each peer algorithm [41, 42]. Table 13 presents the results of each post hoc analysis in terms of z values, unadjusted p-values, and adjusted p-values. It is observed that all post hoc analyses have validated that GTO can outperform AOA and PSO significantly in terms of surface roughness value because all adjusted p-values obtained are smaller than $\sigma = 0.05$. If the threshold significance level is adjusted to $\sigma = 0.10$, GTO is verified by all post hoc analyses to perform significantly better than GWO. Finally, both of Holm and Hochberg analyses can verify the significant performance of GTO against SCA when $\sigma = 0.10$.

Table 12: Friedman test for the multiple comparison between GTO and its peer algorithms.

Algorithm compared with GTO	Ranking	Chi-square statistic	p-value
PSO	4.825		
DE	3.225		
TLBO	2.775		
GWO	4.325	$3.99E+01$	$0.00E+00$
SCA	4.1		
AOA	6.125		
GTO	2.625		

Table 13: Post hoc analyses for the multiple comparison between GTO and its peer algorithms.

Algorithm compared with GTO	Unadjusted p	Bonferroni-Dunn p	Holm p	Hochberg p
AOA	0.000000	0.000002	0.000002	0.000002
PSO	0.001280	0.007679	0.006399	0.006399
GWO	0.012827	0.076960	0.051307	0.051307
SCA	0.030836	0.185018	0.092509	0.092509
DE	0.379775	2.278653	0.759551	0.759551
TLBO	0.826200	4.957201	0.826200	0.826200

4. Conclusion

This research was aimed at using an emerging metaheuristic algorithm known as Gorilla Troops Optimizer (GTO) to solve WEDM machining problem by searching for the optimal machining parameters that can lead to the best (i.e., lowest) surface finish.

The machining of aluminum alloy was done with brass wire as a cathode tool and deionised water as a dielectric medium. ANFIS was used to generate about 500 datasets from 27 experimental datasets. On the contrary to many existing metaheuristic search algorithms, GTO has two different optimization phases with five search operators. It was able to search for the optimal machining parameters in solution space effectively and efficiently without having large population number. At the end of optimization processes, the optimal machining parameters as stored in silverback solution of GTO were pulse-on time = 121 μs, pulse-off time = 52 μs, wire feed = 3 m/min, and current value = 166 A. These parameters are the best process parameters to achieve the minimum surface roughness of 0.500953 microns.

The current metaheuristic algorithm was able to solve WEDM machining problem in 20 independent simulation runs with small standard deviation value of $SD = 0.0060295$, implying the high consistency of the algorithm to search for the optimal machining parameters. Various statistical analyses such as Wilcoxon signed rank test, Friedman test, and post hoc analyses were also performed to verify the significant performance gain of GTO against other metaheuristic search algorithms when solving the current machining problem. To ensure the practicability of optimization results produced by GTO, validation experiments were also performed and found deviation of $\Delta = 0.2\%$ between the predicted and measured surface roughness values. The negligible error value implies the feasibility of GTO to solve real-world WEDM machining optimization problems.

Nomenclature

ANFIS: Adaptive Neurofuzzy Inference System
WEDM: Wire cut electric discharge machining
GRA: Grey rational analysis
HSS: High speed steel
MQL: Minimum quantity lubrication
MRR: Material removal rate
EWR: Electrode wear rate
OC: Overcut
RSM: Response surface model
ARAS: Additive ratio assessment
AHP: Analytic hierarchy process
TOPSIS: Technique for order preference by similarity to ideal situation
BBD: Box-Behnken design
MOPSO: Multiobjective particle swarm optimization
GTO: Gorilla Troops Optimizer
DoE: Design of experiment
ANN: Artificial neural network
MF: Membership function
trimf: Triangular shaped membership function
trapmf: Trapezoidal-shaped membership function
gbellmf: Generalized bell-shaped membership function
gaussmf: Gaussian curve membership function
gauss2mf: Gaussian combination membership function
pimf: P-shaped membership function
dsigmf: Difference between two sigmoidal membership functions
psigmf: Product of two sigmoid membership functions
gbellmf: Generalized bell-shaped membership function
RMSE: Root mean square error
PSO: Particle swarm optimization
DE: Differential evolution
TLBO: Teaching learning-based optimization
GWO: Grey wolf optimizer
SCA: Sine cosine algorithm
AOA: Arithmetic optimization algorithm

Indices

i: Population index of gorilla in GTO
d: Dimension index
t: Iteration index
$\cos(\bullet)$: Cosine operator
$F[\bullet]$: Operator used to calculate the fitness value of a given position value
$O(\bullet)$: Complexity of algorithm estimated using Big-O notation

Parameter and Variables

P_1: Pulse-on time
P_2: Pulse-off time
WF: Servo wire feed
I: Current
R_a: Surface roughness
D: Total dimension size of optimization problem
N: Population size
$X_i(t)$: Position value of ith gorilla at the tth iteration
$x_{i,d}(t)$: Position value of ith gorilla in dth dimension at the tth iteration
r_1, r_2, r_3, r_4, r_5, r_6, rand: Real-valued number within [0, 1] randomly generated from uniform distribution
l: Real-valued number within [-1, 1] randomly generated from uniform distribution.
LB: Lower boundary limits
UB: Upper boundary limits
p: Constant parameter within [0, 1] used to indicate the likelihood of gorilla to migrate towards unknown places
$X_r(t)$: Position value of a randomly selected gorilla at the tth iteration
$GX_r(t)$: Candidate position value of a randomly selected gorilla at the tth iteration
$GX_i(t)$: Candidate position value of ith gorilla at the tth iteration
C: Search range of gorilla
L: Variation of silverback's leadership
T_{max}: Maximum iteration numbers
W: Parameter used to determine the behavior of gorilla in exploitation phase
M: Mean position of gorilla population
Q: Impact force
A: Degree of violence encountered by gorilla in competition
β: Constant parameter used to determine violence effect of gorilla
E: Parameter used to simulate the violence effect on each dimension of solution
N_1, N_2: Normal distributions used to model the violence effect
ω: Inertia weight of particle swarm optimization
c_1, c_2: Acceleration coefficient of particle swarm optimization
F: Scaling factor of differential evolution
CR: Crossover rate of differential evolution
T_f: Teaching factor of teaching learning based optimization
a: Convergence coefficient of grey wolf optimizer
A_{SCA}: Constant used to balance exploration and exploitation of sine cosine algorithm
μ: Control parameter used to adjust the search process of arithmetic optimization algorithm
α: Control parameter used to define exploitation accuracy of arithmetic optimization algorithm over iterations
T_{best}: Iteration number consumed by an algorithm to achieve best result
SD: Standard deviation
σ: Significant level of nonparametric statistical procedures
R^+: Sum of rank for GTO to perform better than a given competing algorithm
R^-: Sum of rank for GTO to perform worse than a given competing algorithm.

Data Availability

The data associated with this research can be obtained from the corresponding author upon request.

Conflicts of Interest

The authors declare that there are no conflicts of interest.

References

[1] N. Z. Khan, Z. A. Khan, A. N. Siddiquee, and A. K. Chanda, "Investigations on the effect of wire EDM process parameters on surface integrity of HSLA: a multi-performance characteristics optimization," *Production & Manufacturing Research*, vol. 2, no. 1, pp. 501–518, 2014.

[2] J. A. Abbasi, M. Jahanzaib, M. Azam, S. Hussain, A. Wasim, and M. Abbas, "Effects of wire-cut EDM process parameters on surface roughness of HSLA steel," *International Journal of Advanced Manufacturing Technology*, vol. 91, no. 5-8, pp. 1867–1878, 2017.

[3] Y. Takayama, Y. Makino, Y. Niu, and H. Uchida, "The latest technology of wire-cut EDM," *Procedia CIRP*, vol. 42, pp. 623–626, 2016.

[4] I. Ayesta, O. Flaño, B. Izquierdo, J. A. Sanchez, and S. Plaza, "Experimental study on debris evacuation during slot EDMing," *Procedia CIRP*, vol. 42, pp. 6–11, 2016.

[5] J. Singh and R. K. Sharma, "Assessing the effects of different dielectrics on environmentally conscious powder-mixed EDM of difficult-to-machine material (WC-Co)," *Frontiers of Mechanical Engineering*, vol. 11, no. 4, pp. 374–387, 2016.

[6] L. Liu, M. Qiu, C. Shao, M. Zhang, and J. Zhao, "Research on wire-cut electrical discharge machining constant discharge probability pulse power source for silicon crystals,"

International Journal of Advanced Manufacturing Technology, vol. 100, no. 5-8, pp. 1815–1824, 2019.

[7] A. Muniappan, C. Thiagarajan, P. V. Senthiil, V. Jayakumar, and T. Shaafi, "Effect of wire-EDM process parameters on cutting speed of AL6061 hybrid composite," *International Journal of Mechanical Engineering & Technology*, vol. 8, no. 10, pp. 185–189, 2017.

[8] M. S. Alsoufi and D. K. Suker, "Experimental investigation of wire-EDM process parameters for surface roughness in the machining of carbon steel 1017 and aluminum alloy 6060," *American Journal of Mechanical Engineering*, vol. 6, no. 3, pp. 132–147, 2018.

[9] A. Kumar, T. Soota, and J. Kumar, "Optimisation of wire-cut EDM process parameter by Grey-based response surface methodology," *Journal of Industrial Engineering International*, vol. 14, no. 4, pp. 821–829, 2018.

[10] A. Pramanik and A. K. Basak, "Sustainability in wire electrical discharge machining of titanium alloy: understanding wire rupture," *Journal of Cleaner Production*, vol. 198, pp. 472–479, 2018.

[11] S. K. Shihab, "Optimization of WEDM process parameters for machining of friction-stir-welded 5754 aluminum alloy using Box–Behnken design of RSM," *Arabian Journal for Science and Engineering*, vol. 43, no. 9, pp. 5017–5027, 2018.

[12] H. Hegab, H. A. Kishawy, and B. Darras, "Sustainable cooling and lubrication strategies in machining processes: a comparative study," *Procedia Manufacturing*, vol. 33, pp. 786–793, 2019.

[13] P. Nagarajan, P. K. Murugesan, and E. Natarajan, "Optimum control parameters during machining of LM13 aluminum alloy under dry electrical discharge machining (EDM) with a modified tool design," *Materials Science*, vol. 25, no. 4, pp. 407–412, 2019.

[14] T. Chaudhary, A. N. Siddiquee, and A. K. Chanda, "Effect of wire tension on different output responses during wire electric discharge machining on AISI 304 stainless steel," *Defence Technology*, vol. 15, no. 4, pp. 541–544, 2019.

[15] S. Ramesh, N. Vijayakumar, and E. Natarajan, "Electrical discharge machining analysis of zirconium powder mixed dielectric on performance of high carbon high chromium steel," *Journal of the Balkan Tribological Association*, vol. 26, no. 1, pp. 165–192, 2020.

[16] R. Chaudhari, J. Vora, D. M. Parikh, V. Wankhede, and S. Khanna, "Multi-response optimization of WEDM parameters using an integrated approach of RSM–GRA analysis for pure titanium," *Journal of the Institution of Engineers*, Series D, vol. 101, pp. 117–126, 2020.

[17] A. Ramaswamy, A. V. Perumal, and A. V. Perumal, "Multi-objective optimization of drilling EDM process parameters of LM13 al alloy–10ZrB2–5TiC hybrid composite using RSM," *Journal of the Brazilian Society of Mechanical Sciences and Engineering*, vol. 42, no. 8, p. 432, 2020.

[18] T. Sathish, V. Mohanavel, K. Ansari et al., "Synthesis and characterization of mechanical properties and wire cut EDM process parameters analysis in AZ61 magnesium alloy + B4C + SiC," *Materials*, vol. 14, no. 13, p. 3689, 2021.

[19] J. U. Prakash, P. Sivaprakasam, I. Garip et al., "Wire electrical discharge machining (WEDM) of hybrid composites (Al-Si12/B_4C/Fly Ash)," *Journal of Nanomaterials*, vol. 2021, pp. 1–10, 2021.

[20] N. R. J. Hynes, D. S. S. P. Kumar, M. V. Prabhu, M. A. Ali, M. H. Raza, and C. I. Pruncu, "Investigating the parametric effects on wire electric discharge machining performance in processing AA1050-5 wt.% SiC composite with zinc-coated brass wire," *Journal of the Brazilian Society of Mechanical Sciences and Engineering*, vol. 44, no. 4, p. 127, 2022.

[21] V. Aggarwal, C. I. Pruncu, J. Singh, S. Sharma, and D. Y. Pimenov, "Empirical investigations during WEDM of Ni-27Cu-3.15Al-2Fe-1.5Mn based superalloy for high temperature corrosion resistance applications," *Materials*, vol. 13, no. 16, p. 3470, 2020.

[22] B. Sen, S. A. I. Hussain, A. D. Gupta, M. K. Gupta, D. Y. Pimenov, and T. Mikołajczyk, "Application of type-2 fuzzy AHP-ARAS for selecting optimal WEDM parameters," *Metals*, vol. 11, no. 1, p. 42, 2020.

[23] T. Mikolajczyk, "Analyse of possibility of form tools manufacturing using wire cutting EDM," *Applied Mechanics and Materials*, vol. 656, pp. 200–205, 2014.

[24] K. Fuse, A. Dalsaniya, D. Modi et al., "Integration of fuzzy AHP and fuzzy TOPSIS methods for wire electric discharge machining of titanium (Ti6Al4V) alloy using RSM," *Materials*, vol. 14, no. 23, p. 7408, 2021.

[25] K. K. Goyal, N. Sharma, R. Dev Gupta et al., "A soft computing-based analysis of cutting rate and recast layer thickness for AZ31 alloy on WEDM using RSM-MOPSO," *Materials*, vol. 15, no. 2, p. 635, 2022.

[26] M. N. Alam, A. N. Siddiquee, Z. A. Khan, and N. Z. Khan, "A comprehensive review on wire EDM performance evaluation," *Proceedings of the Institution of Mechanical Engineers - Part E: Journal of Process Mechanical Engineering*, Article ID 095440892210748, 2022.

[27] M. H. Abidi, A. M. Al-Ahmari, U. Umer, and M. S. Rasheed, "Multi-objective optimization of micro-electrical discharge machining of nickel-titanium-based shape memory alloy using MOGA-II," *Measurement*, vol. 125, pp. 336–349, 2018.

[28] S. Suresh, N. Elango, K. Venkatesan, W. H. Lim, K. Palanikumar, and S. Rajesh, "Sustainable friction stir spot welding of 6061-T6 aluminium alloy using improved non-dominated sorting teaching learning algorithm," *Journal of Materials Research and Technology*, vol. 9, no. 5, pp. 11650–11674, 2020.

[29] P. Kayaroganam, V. Krishnan, E. Natarajan, S. Natarajan, and K. Muthusamy, "Drilling parameters analysis on in-situ al/b4 c/mica hybrid composite and an integrated optimization approach using fuzzy model and non-dominated sorting genetic algorithm," *Metals*, vol. 11, no. 12, p. 2060, 2021.

[30] S. Elango, K. Varadaraju, E. Natarajan, E. M. Abraham Gnanamuthu, R. Durairaj, and P. Mariappan, "PTFE in wet and dry drilling: two-tier modeling and optimization through ANFIS," *Mathematical Problems in Engineering*, vol. 2022, pp. 1–10, 2022.

[31] B. Abdollahzadeh, F. Soleimanian Gharehchopogh, and S. Mirjalili, "Artificial gorilla troops optimizer: a new nature-inspired metaheuristic algorithm for global optimization problems," *International Journal of Intelligent Systems*, vol. 36, no. 10, pp. 5887–5958, 2021.

[32] I. Ahmed, A. Dahou, S. A. Chelloug, M. A. A. Al-Qaness, and M. A. Elaziz, "Feature selection model based on gorilla troops optimizer for intrusion detection systems," *Journal of Sensors*, vol. 2022, Article ID 6131463, 12 pages, 2022.

[33] G. I. Sayad and A. E. Hassanien, "A novel chaotic artificial gorilla troops optimizer and its application for fundus images segmentation," in *Proceedings of the International Conference on Advanced Intelligent Systems and Informatics 2021. AISI 2021. Lecture Notes on Data Engineering and Communications Technologies*, A. E. Hassanien, V. Snášel, KC. Chang, A. Darwish, and T. Gaber, Eds., vol. 100, 2022.

[34] A. H. Yakout, H. Kotb, K. M. AboRas, and H. M. Hasanien, "Comparison among different recent metaheuristic algorithms for parameters estimation of solid oxide fuel cell: steady-state and dynamic models," *Alexandria Engineering Journal*, vol. 61, no. 11, pp. 8507–8523, 2022.

[35] A. Ginidi, S. M. Ghoneim, A. Elsayed, R. El-Sehiemy, A. Shaheen, and A. El-Fergany, "Gorilla troops optimizer for electrically based single and double-diode models of solar photovoltaic systems," *Sustainability*, vol. 13, no. 16, p. 9459, 2021.

[36] J. Kennedy and R. Eberhart, "Particle swarm optimization," in *Proceedings of ICNN'95 - International Conference on Neural Networks*, Perth, WA, Australia, December 1995.

[37] R. Storn and K. Price, "Differential evolution – a simple and efficient heuristic for global optimization over continuous spaces," *Journal of Global Optimization*, vol. 11, no. 4, pp. 341–359, 1997.

[38] S. Mirjalili, S. M. Mirjalili, and A. Lewis, "Grey wolf optimizer," *Advances in Engineering Software*, vol. 69, pp. 46–61, 2014.

[39] S. Mirjalili, "SCA: a Sine Cosine Algorithm for solving optimization problems," *Knowledge-Based Systems*, vol. 96, pp. 120–133, 2016.

[40] L. Abualigah, A. Diabat, S. Mirjalili, M. Abd Elaziz, and A. H. Gandomi, "The arithmetic optimization algorithm," *Computer Methods in Applied Mechanics and Engineering*, vol. 376, Article ID 113609, 2021.

[41] S. García, D. Molina, M. Lozano, and F. Herrera, "A study on the use of non-parametric tests for analyzing the evolutionary algorithms' behaviour: a case study on the CEC'2005 Special Session on Real Parameter Optimization," *Journal of Heuristics*, vol. 15, no. 6, pp. 617–644, 2009.

[42] J. Derrac, S. García, D. Molina, and F. Herrera, "A practical tutorial on the use of nonparametric statistical tests as a methodology for comparing evolutionary and swarm intelligence algorithms," *Swarm and Evolutionary Computation*, vol. 1, no. 1, pp. 3–18, 2011.